

University of Groningen

New Therapeutic Approach for Intestinal Fibrosis Through Inhibition of pH-Sensing Receptor GPR4

Weder, Bruce; Schefer, Fabian; van Haaften, Wouter Tobias; Patsenker, Eleonora; Stickel, Felix; Mueller, Sebastian; Hutter, Senta; Schuler, Cordelia; Baebler, Katharina; Wang, Yu

Published in:
Inflammatory Bowel Diseases

DOI:
[10.1093/ibd/izab140](https://doi.org/10.1093/ibd/izab140)

IMPORTANT NOTE: You are advised to consult the publisher's version (publisher's PDF) if you wish to cite from it. Please check the document version below.

Document Version
Publisher's PDF, also known as Version of record

Publication date:
2022

[Link to publication in University of Groningen/UMCG research database](#)

Citation for published version (APA):

Weder, B., Schefer, F., van Haaften, W. T., Patsenker, E., Stickel, F., Mueller, S., Hutter, S., Schuler, C., Baebler, K., Wang, Y., Mamie, C., Dijkstra, G., de Vallière, C., Imenez Silva, P. H., Wagner, C. A., Frey-Wagner, I., Ruiz, P. A., Seuwen, K., Rogler, G., & Hausmann, M. (2022). New Therapeutic Approach for Intestinal Fibrosis Through Inhibition of pH-Sensing Receptor GPR4. *Inflammatory Bowel Diseases*, 28(1), 109-125. <https://doi.org/10.1093/ibd/izab140>

Copyright

Other than for strictly personal use, it is not permitted to download or to forward/distribute the text or part of it without the consent of the author(s) and/or copyright holder(s), unless the work is under an open content license (like Creative Commons).


The publication may also be distributed here under the terms of Article 25fa of the Dutch Copyright Act, indicated by the "Taverne" license. More information can be found on the University of Groningen website: <https://www.rug.nl/library/open-access/self-archiving-pure/taverne-amendment>.

Take-down policy

If you believe that this document breaches copyright please contact us providing details, and we will remove access to the work immediately and investigate your claim.

Downloaded from the University of Groningen/UMCG research database (Pure): <http://www.rug.nl/research/portal>. For technical reasons the number of authors shown on this cover page is limited to 10 maximum.

New Therapeutic Approach for Intestinal Fibrosis Through Inhibition of pH-Sensing Receptor GPR4

Bruce Weder, PhD,^{*,**} Fabian Schefer,^{*,**} Wouter Tobias van Haaften, MD, PhD,^{†,‡}
Eleonora Patsenker, PhD,^{*} Felix Stickel, MD,^{*} Sebastian Mueller, MD, PhD,[§] Senta Hutter, MD,^{*}
Cordelia Schuler,^{*} Katharina Baebler,^{*} Yu Wang, PhD,^{*} Céline Mamie,^{*} Gerard Dijkstra, MD, PhD,[†]
Cheryl de Vallière, PhD,^{*} Pedro H. Imenez Silva, PhD,[¶] Carsten A. Wagner, MD,[¶]
Isabelle Frey-Wagner, PhD,^{*} Pedro A. Ruiz, PhD,^{*} Klaus Seuwen, PhD,^{||} Gerhard Rogler, MD, PhD,^{*}
and Martin Hausmann, PhD^{*} 

From the ^{*}Department of Gastroenterology and Hepatology, University Hospital Zurich, Zurich, Switzerland

[†]Department of Gastroenterology and Hepatology, University Medical Center Groningen, University of Groningen, Groningen, the Netherlands

[‡]Department of Pharmaceutical Technology and Biopharmacy, Groningen Research Institute of Pharmacy, University of Groningen, Groningen, the Netherlands

[§]Department of Internal Medicine and Center for Alcohol Research, Salem Medical Center University Hospital Heidelberg, Heidelberg, Germany

[¶]Institute of Physiology, University of Zurich, Zurich, Switzerland and National Center of Competence in Research Kidney Control of Homeostasis, Switzerland

^{||}Novartis Institutes for Biomedical Research, Forum1 Novartis Campus, Basel, Switzerland

^{**}Equal contribution.

Address correspondence to: Martin Hausmann, PhD, Department of Gastroenterology and Hepatology, University Hospital Zurich, 8091 Zurich, CH-Switzerland. E-mail: Martin.Hausmann@usz.ch.

Background: Patients suffering from inflammatory bowel diseases (IBDs) express increased mucosal levels of pH-sensing receptors compared with non-IBD controls. Acidification leads to angiogenesis and extracellular matrix remodeling. We aimed to determine the expression of pH-sensing G protein-coupled receptor 4 (GPR4) in fibrotic lesions in Crohn's disease (CD) patients. We further evaluated the effect of deficiency in *Gpr4* or its pharmacologic inhibition.

Methods: Paired samples from fibrotic and nonfibrotic terminal ileum were obtained from CD patients undergoing ileocaecal resection. The effects of *Gpr4* deficiency were assessed in the spontaneous *Il-10*^{-/-} and the chronic dextran sodium sulfate (DSS) murine colitis model. The effects of *Gpr4* deficiency and a GPR4 antagonist (39c) were assessed in the heterotopic intestinal transplantation model.

Results: In human terminal ileum, increased expression of fibrosis markers was accompanied by an increase in GPR4 expression. A positive correlation between the expression of procollagens and GPR4 was observed. In murine disease models, *Gpr4* deficiency was associated with a decrease in angiogenesis and fibrogenesis evidenced by decreased vessel length and expression of *Edn*, *Vegfa*, and procollagens. The heterotopic animal model for intestinal fibrosis, transplanted with terminal ileum from *Gpr4*^{-/-} mice, revealed a decrease in mRNA expression of fibrosis markers and a decrease in collagen content and layer thickness compared with grafts from wild type mice. The GPR4 antagonist decreased collagen deposition. The GPR4 expression was also observed in human and murine intestinal fibroblasts. The GPR4 inhibition reduced markers of fibroblast activation stimulated by low pH, notably Acta2 and *cTgf*.

Conclusions: Expression of GPR4 positively correlates with the expression of profibrotic genes and collagen. Deficiency of *Gpr4* is associated with a decrease in angiogenesis and fibrogenesis. The GPR4 antagonist decreases collagen deposition. Targeting GPR4 with specific inhibitors may constitute a new treatment option for IBD-associated fibrosis.

Key Words: acidification, angiogenesis, inflammatory bowel disease

Abbreviations: ACTA2, α -smooth muscle actin; ASMC, airway smooth muscle cells; ACTB, beta-actin; bFGF, basic fibroblast growth factor; cAMP, cyclic adenosine monophosphate; CD, Crohn's disease; COL1A1, procollagen type 1 alpha 1; COL1A2, procollagen type 1 alpha 2; COL3A1, procollagen type III alpha 1; COL5A1, procollagen type V alpha 1; COL12A1, procollagen type XII alpha 1; COL16A1, procollagen type XVI alpha 1; CTGF, connective tissue growth factor; DEF, defensin; FN, fibronectin; GAPDH, glyceraldehyde-3-phosphate dehydrogenase; OGR1/GPR68, G-protein coupled receptor 1; GPR, G-protein coupled receptor; HPRT, hypoxanthine phosphoribosyltransferase 1; HYP, 4-hydroxyproline; IBD, inflammatory bowel disease; IF, immunofluorescence; IL, interleukin; IFN γ , interferon γ ; iNOS, inducible nitric oxide synthase; IP1, inositol 1-monophosphate; IP3, inositol 1,4,5-trisphosphate; MCP1, monocyte chemoattractant protein 1; MSC, mesenchymal stem cell; mRNA, messenger RNA; qPCR, real-time quantitative polymerase chain reaction; TDAG8/GPR65, T cell death-associated gene 8; TGF β 1, transforming growth factor β 1; TNF, tumor necrosis factor; UC, ulcerative colitis; VIM, vimentin; WB, western blot

Introduction

Intestinal inflammation in both ulcerative colitis (UC) and Crohn's disease (CD), the main forms of inflammatory bowel disease (IBD), are associated with mucosal acidity due to

increased local proton concentration, low oxygen concentration, excessive production and insufficient elimination of glycolytic metabolites (eg, lactic acid),^{1–4} and subsequent pro-inflammatory cytokine production.⁴ Therefore, an acidic

environment is not only the result of inflammation but also affects the degree and outcome of inflammation.⁵⁻⁷ Excessive tissue repair causes fibrosis and impairs gastrointestinal function. Intestinal fibrosis is a common clinical problem in patients with CD and UC,⁸ which often leads to stricture formation due to thickening of the intestinal wall in 30% to 50% of CD patients. Approximately 80% of patients with stricturing CD will eventually require surgery.⁹⁻¹¹ Acidification and pH-dependent signaling is relevant for the induction of inflammation and for the development of fibrosis in severe asthma and irreversible airway obstruction.^{12,13}

Three G protein-coupled receptors (GPCRs) from the GPR4 subfamily have been identified as sentinels for proton concentration, as they enable cells to sense the surrounding pH and respond to it.^{14,15} This subfamily includes GPR4, ovarian cancer G protein-coupled receptor 68 (OGR1/*GPR68*) and T cell death-associated gene 8 (*TDAG8/GPR65*). These receptors sense extracellular protons through histidine residues located in the extracellular domains of the receptor, resulting in signaling pathway activation and the modification of numerous cell functions. The proton-sensing receptors *TDAG8*, *OGR1*, and *GPR4* are inactive or only slightly active in an alkaline environment (pH 7.6–7.8) but become highly activated in acidic environments (pH 6.8).^{7,15-17}

A growing body of literature links *GPR4* to angiogenesis, a process closely associated with fibrosis. The inflammatory activity in CD is characterized by an increased vessel density and angiogenesis,^{18,19} by which the local microvasculature undergoes an intense process of inflammation-dependent angiogenesis associated with increased levels of vascular endothelial growth factor (VEGF). Mice deficient in *GPR4* show a significantly reduced angiogenic response to VEGF in a growth factor implant model,²⁰ which indicates that sensing tissue acidosis through *GPR4* by endothelial cells is required for VEGF action. Vascular endothelial growth factor signaling is considered to be pro-inflammatory and profibrotic and triggers fibroblast to myofibroblast transformation through the induction of transforming growth factor (TGF) β 1, as shown for subconjunctival²¹ and kidney fibrosis.²² Expression of pH-sensing receptors *OGR1* and *TDAG8* has also been reported in macrophages,^{23,24} smooth muscle cells,^{23,24} T cells,²⁴ and fibroblasts.²⁴

Orally active *GPR4* antagonists for the treatment of inflammatory diseases and pain were recently developed.²⁵ The *GPR4* inhibitor compound 13 was shown to inhibit intestinal inflammation in a murine acute colitis model.²⁶ The *GPR4* targeting compound 39c was tested in animal models of angiogenesis, arthritis, and pain.²⁵ Oral application of compound 39c inhibited VEGF-induced angiogenesis and knee swelling in an antigen-induced arthritis model with an efficacy similar to dexamethasone and an analgesic effect comparable to the NSAID diclofenac.²⁵

In the present study, we determined the expression of *GPR4* in intestinal fibrotic lesions of patients with CD compared with nonfibrotic control sections. Our results show that the expression of *GPR4* correlates with profibrotic gene expression and collagen deposition. We studied the impact of *GPR4* deficiency in 3 different animal models of intestinal fibrosis: the dextran sodium sulfate (DSS) chronic colitis model, the interleukin (*Il*)-10^{-/-} mouse model of spontaneous colitis, and a heterotopic transplantation model of intestinal fibrosis. We report that *Gpr4* deficiency (*Gpr4*^{-/-}) leads to a decrease in

angiogenesis and fibrogenesis. Moreover, the presence of the *GPR4* antagonist decreased collagen deposition in the studied mouse models of intestinal fibrosis. Our results from in vitro assays show that low pH enhances fibroblast differentiation and *GPR4* inhibition reduces mesenchymal cell activation. Inhibition of *GPR4* may represent a new treatment option for IBD-associated fibrosis.

Materials and Methods

Ethical Considerations

We obtained ethical approval to examine intestinal samples and use patient data from Netherland residents diagnosed with IBD. Patients gave written informed consent for anonymous use of patient data and resections according to the code of conduct for responsible use of surgical leftover material (www.rug.nl/umcg/research/documents/research-code-info-umcg-nl.pdf).

We also obtained ethical approval to isolate mucosal cells from intestinal samples and use patient data from a cohort study of Swiss residents diagnosed with IBD from the local ethical committee of the canton of Zurich (EK-1316).

Human Tissue from Patients

Paired intestinal tissue samples from Netherland residents, namely thickened fibrosis-affected regions and nonfibrosis-affected resection margins (Supplementary Table 1), were obtained from patients with CD undergoing ileocecal resection due to stenosis in the terminal ileum. Coincidentally, all patients with CD were female. Immediately after resection, samples for transcriptomic analysis were fixed in Tissue-Tek (Sakura, Alphen aan den Rijn, Netherlands) in the operation room and frozen in isopentane on dry ice. Samples were stored at -80 °C until further use.

Intestinal epithelial crypts were isolated from Swiss residents (Supplementary Table 2). Human colonic mucosa from surgical specimens was cut in to small strips (5 mm). Mucus was removed by incubating the strips for 30 minutes at room temperature in Hanks' balanced salt solution (HBSS; Sigma-Aldrich, Switzerland) supplemented with 1 mM 1,4-dithiothreitol (DTT; Sigma-Aldrich). The strips were subsequently agitated in HBSS containing 1 mM EDTA (Sigma-Aldrich) for 10 minutes at 37°C, vigorously shaken for 10 times, and passed over a coarse mesh (400 μ m, Carl Roth, Germany). Sieve throughput was discarded. Shaking and sieving was repeated 3 times and intestinal epithelial cells in the thorough fractions were collected. The crypt-containing and single cell-containing suspension was filtered through a 70- μ m cell strainer (BD Biosciences). Intact colonic crypts were retained in the cell strainer and eluted by inverting the cell strainer in Dulbecco's Modified Eagle Medium (DMEM; Invitrogen, Switzerland) containing 10% fetal bovine serum (PAA Laboratories, Germany).

Animals

The animal experiment protocol was approved by the Veterinary Authority of the canton of Zurich (registration number ZH242/2016).

Gain-of-function transgenic mice that are able to express GFP in *GPR4*⁺ cells were generated by targeting the murine *GPR4* gene and the *Rosa26* locus. For the generation of B6.C-Gpr4 < tm1(CreN) Npa > x B6.C-Gt(ROSA)26Sor < tm2(CAG-EGFP)Npa, cross-

breeding was performed using the following 2 strains obtained from Novartis: BB6.C-Gpr4 <tm1(CreN)Npa > contains a targeted mutation of the murine Gpr4 gene as previously described²⁷; the Gpr4 ORF was replaced by the gene-coding for cre recombinase. This allows expression of cre recombinase in Gpr4-expressing cells. BB6.C-Gt(ROSA)26Sor <tm2(CAG-EGFP)Npa allows cre-inducible expression of GFP from the Rosa26 locus as previously described.²⁸ Both lines were originally generated on BALB/c background and then backcrossed to C57BL/6 background. Mice heterozygous for both mutations were used for the experiment. Expression of GPR4 was analyzed throughout the gut using anti-GFP immunohistochemistry.

Animal experiments were performed according to the ARRIVE criteria. The generation, breeding, and genotyping of *Gpr4*^{-/-} and *Gpr4*^{-/-}/*Il-10*^{-/-} (BALB/c and C57BL/6) mice have been previously described.²³ Littermates were used in all experiments involving transgenic mice. The animals were cohoused to minimize potential effects of microbiota variation. The C57BL/6 wild type (WT) mice were obtained from the Jackson Laboratory, Bar Harbor, ME, United States.

Induction of Colitis With DSS

Female mice between 10 and 13 weeks of age and with a body weight around 20 g were used in the experiment. Colitis was induced with DSS (MP Biomedicals, LLC, Solon, OH, USA), as previously described.²³ Briefly, for acute colitis, mice were administered with 3% DSS in drinking water ad libitum for 7 days. For chronic colitis, WT and *Gpr4*^{-/-} mice were administered with 4 cycles of 3% DSS in drinking water ad libitum for 7 days followed by 10 days of regular drinking water. After the last cycle, all animals were allowed to recover for 5 weeks and subsequently were sacrificed for sample collection. Mice on regular drinking water served as controls throughout the experiment. Data for the DSS model of chronic colitis originated from 3 rounds of experiments with mice with an identical genetic background (littermates).

Spontaneous Colitis in *Il-10*^{-/-} Mice

In the spontaneous *Il-10*-deficient colitis model, the onset and development of inflammatory markers, colitis, and rectal prolapses were monitored over 80 days, as previously described.²³

Heterotopic Intestinal Transplant Model

Female mice used for the experiment weighed 19 to 23 g and were 10 to 16 weeks old when the experiment was started. The heterotopic mouse intestinal transplant model has been previously described in detail.²⁹ Briefly, a 30 to 40-mm small bowel proximal to the cecum section from donor mice was excised and implanted into a subcutaneous pouch into the neck of recipient mice. A single dose of Cefazolin (Kefzol) was administered IP. Grafts were explanted 6 days after transplantation.

The GPR4 antagonist (compound 39c, Novartis) was diluted in 0.9% NaCl and applied IP in a dose-dependent manner (vehicle, 3, 10, and 30 mg per kg mouse weight). The GPR4 antagonist was applied 3 times daily for 7 days starting on the day of transplantation. Pirfenidone was diluted in 0.9% NaCl and applied IP at 100 mg per kg mouse weight, 3 times daily.

RNA Isolation and Real-time Quantitative Polymerase Chain Reaction

To isolate RNA from the human intestinal samples from Netherland residents, ten 10- μ m-thick Tissue-Tek sections containing full cross-sections of the intestinal wall were cut using a cryostat. These sections were dissolved and homogenized in TRIzol (15596018, Invitrogen, Life Technologies). The total RNA was isolated according to the manufacturer's protocol. To avoid genomic DNA contamination, samples were treated with DNase 1 (18068 015, Amp Grade, Invitrogen, Life Technologies, Carlsbad, CA, United States) according to the manufacturer's protocol.

RNA isolation from human mucosa and crypts from Swiss residents and RNA isolation from murine specimens were performed following the instructions of the RNeasy Mini Kit (74104, Qiagen, Switzerland).

RNA isolation of cell cultures was performed following the instructions of the Maxwell RSC simply RNA Kit (AS1340, Promega, Switzerland).

Real-time quantitative polymerase chain reaction (RT-qPCR) was performed using TaqMan gene expression assays (Thermo Fisher Scientific, Switzerland) for *ACTA2* Hs00426835_g1, *COL1A1* Hs00164004_m1, *COL1A2* Hs01028956_m1, *COL3A1* Hs00943809_m1, *CTGF* Hs00170014_m1, *DEFA5* Hs00360716_m1, *DEFA6* Hs00236950_m1, *GAPDH* 4326317E, *GPR4* Hs00270999_s1, *HIF1 α* Hs00936370_m1, *ICAM1* Hs00164932_m1, *VIM* Hs00185584_m1, *Acta2* Mm01546133_m1, *Cd80* Mm00711660_m1, *Cd86* Mm00444543_m1, *Col1a1* Mm00801666_g1, *Col1a2* Mm00483888_m1, *Col3a1* Mm01254476_m1, *Col5a1* Mm00489299_m1, *Col12a1* Mm01148576_m1, *Col16a1* Mm01180622_m1, *cTgf* Mm01192933_g1, *Edn* Mm00438659_m1, *Eln* Mm00514670_m1, *Fkbp10* Mm00487407_m1, *Fn1* Mm01256744_m1, *Has2* Mm00515089_m1, *Il-1 β* Mm01336189_m1, *Pdgfr β* Mm00440677_m1, *Tgf* Mm01178820_m1, *Vegfa* Mm00437306_m1, *Vim* Mm01333430_m1, and *Gapdh* 4352339E. Relative gene expression was calculated using the $\Delta\Delta$ Ct-method.

Vessel Count

Vessels stained for CD31 were counted. Pictures at 20x magnification using the Imager Z2 microscope and the software ZEN (Zeiss, Oberkochen, Germany) were taken encompassing the whole mucosa—defined as the area above the muscularis mucosae—and the submucosa—defined as the area between the muscularis mucosae and muscularis propria. The area of the counted regions was measured using image processing package Fiji/ImageJ (1.47t, NIH, USA). Complete colons from 3 mice per group were counted.

To assess vascular integrity, the length of continuous CD31-stained structures was determined on micrographs from the whole lamina propria at 20x magnification. Values (μ m) were obtained for all vascular structures per group. Structures smaller than 5 μ m and structures in connection with only 1 nucleus were not taken into account.

Sirius Red Staining and Collagen Layer Thickness Measurement

Sections 3 to 5 μ m in length were stained with Sirius Red according to a standard protocol.³⁰ Staining was examined

using the Imager Z2 microscope and the software ZEN. The quantity of collagen was analyzed by Fiji using pictures taken under transmission light or polarized light. Composite images (5x) showing either the entire cross section or cropped 20x magnification pictures from representative areas were taken. By setting a threshold to select the red color (Hue > 220) in areas completely covered with tissue, the presence of collagen was calculated as Hue > 220/total tissue area. Collagen layer thickness was measured by a blinded investigator from at least 8 regions of representative areas at 20x magnification.

Isolation and Culture of Human and Murine Intestinal Fibroblasts

Human fibroblasts were isolated from colonic resections from Swiss residents ([Supplementary Table 3](#)). The mucosa was cut into small blocks of approximately 1 to 2 mm². Petri dishes were gently roughened with a cannula, and the tissue blocks were carefully squeezed onto this support. Blocks were cultured with DMEM containing 10% fetal calf serum (FCS, VWR, Switzerland), penicillin (100 IE/mL, PAA laboratories, Switzerland), streptomycin (100 µg/mL, PAA laboratories), ciprofloxacin (8 µg/mL, Bayer, Germany), gentamycin (50 µg/mL, Chemie Brunschwig AG, Switzerland), and amphotericin B (1 µg/mL, Bristol Myers Squibb, New York, USA). Nonadherent cells were continuously removed. Once cells had migrated out of the block, the excess tissue was removed and the cells were split 3 times using trypsin/EDTA (15400–054, Thermo Fisher Scientific, Perbio Science, Switzerland). Adherent cells were discarded. The remaining cells were used between passages 3 and 8 to minimize changes that might occur in the phenotype of fibroblasts when placed into culture after several passages.

Murine intestinal fibroblasts were isolated from wild type mice with a C57BL/6 background, as described previously.

pHTreatment

The pH shift experiments were carried out in serum-free RPMI-1640 medium supplemented with 2 mM of GlutaMAX and 20 mM of 4-(2-hydroxyethyl)-1-piperazineethanesulfonic acid (HEPES), as previously described.³¹ For pH adjustment of the RPMI medium, the appropriate quantities of NaOH or HCl were added, and the medium was allowed to equilibrate in the 5% CO₂ incubator at 37°C for at least 36 hours before it was used. The pH of all solutions was recorded at the beginning of each experiment. All data presented are referenced to pH measured at room temperature. Cells were starved for 4 to 6 hours in serum-free RPMI medium, pH 7.8, and then subjected to pH shift at various pH values.

Western Blot

Samples were lysed in M-PER protein extraction buffer (Thermo Fisher Scientific). Proteins were separated on 12% polyacrylamide gels with Tris/SDS running buffer and transferred onto nitrocellulose (Invitrogen). Membranes were blocked with 5% milk, 3% bovine serum albumin (BSA) and 0.1% Tween 20 and incubated with polyclonal rabbit antimouse COL1A1 (91144S; Cell Signaling; diluted 1:1'000), monoclonal rabbit antimouse VIM (5741S, Cell Signaling; diluted 1:1'000), polyclonal rabbit antimouse TGFβ1 (3711S,

Cell Signaling; diluted 1:1'000), polyclonal goat antimouse IL-1β (AF-401-NA, Bio-technie, diluted 1:1'000) and polyclonal goat antihuman ACTA2 (NB300–978SS, Novus Biologicals, diluted 1:1'000). Horseradish peroxidase-conjugated secondary antibodies were donkey antigoat (#sc-2020; Santa Cruz; diluted 1:3'000) and goat antirabbit (#sc-2004; Santa Cruz; diluted 1:3'000). Additionally, β-Actin was used as a loading control.

Immunofluorescence

Human intestinal fibroblasts were fixed in 3.7% formaldehyde, washed, and subjected to immunofluorescent staining. Next, 1% BSA in phosphate buffered saline (PBS) was used to block unspecific binding sites. Polyclonal goat antihuman ACTA2 (NB300-978SS, Novus Biologicals, diluted 1:400) was applied. Fluorescent labeling was performed with Alexa Fluor 647 donkey antigoat (#A32849; Invitrogen; diluted 1:1'000). Nuclei were visualized with diamidino phenylindole (D1306, DAPI; Invitrogen; final concentration 3 µM). The sections were mounted with fluorescent mounting medium (S302380, DAKO, Switzerland) and analyzed by confocal laser scanning microscopy (SP5, Leica, Switzerland). The colors were assigned with the help of the software LAS AF lite.

Immunohistochemistry

Specimen were fixed in 4% PBS-buffered formalin, embedded in paraffin and sectioned (3 µm). Immunohistochemistry was performed on a Ventana stainer (Roche, Switzerland), and specimen were stained with hematoxylin using standard histological techniques. GFP was stained with a rabbit polyclonal antibody (20R-GR011, Fitzgerald Industries, 1:1000), ACTA2 with goat polyclonal antibody (ab21027, Abcam, 1:500), CD31 with rabbit polyclonal antibody (ab28364, Abcam, 1:100), F4/80 with monoclonal rat antibody (T-2006, BMA Biomedicals AG, 1:50), and vimentin with goat polyclonal antibody (ab7783, Abcam, 1:800).

RhoA GTPase Activation Assay

Cells were plated in RPMI plus 10% FCS and incubated for 1 hour followed by 2 hours of starvation at pH 7.8 in serum-free RPMI. The pH shift was performed for 1, 5, and 10 minutes at pH 7.4, 6.8 and 6.4. All incubations were carried out in a 5% CO₂ humidified 37°C incubator. Additionally, 15 µg of protein was loaded per well, and GTP-bound RhoA protein levels were measured in duplicates according to the manufacturer's instructions (#BK124, Cytoskeleton, USA). Final absorbance (OD490) was measured in a Synergy 2 microplate reader (Biotek, Luzern, Switzerland).

Statistical Analysis

Statistical analysis was performed as indicated in the figure legends using GraphPad Prism (v5.0). Differences were considered significant at $P < 0.05^*$, as highly significant at $P < 0.01^{**}$ and $P < 0.001^{***}$. Means ± standard deviations are presented. Paired (Fig. 1A, 1C, [Supplementary Fig. 1](#)) and unpaired *t* tests (Figs. 1D, 2B–I, Fig. 3, Fig. 4B, [Supplementary Figs. 2B–D, 3, and 4](#)) were used for comparing the means of 2 samples. Nonparametric Mann-Whitney rank sum was used for nonhomogeneous groups (Fig. 1D, 4C). One-way ANOVA

with post hoc Tukey test was used for comparing multiple treatments (Figs. 2A, 4A, 5B–D, 6D, Supplementary Figs. 2A, 5, and 9).

Results

Expression of GPR4 Is Increased in the Fibrotic Intestine in CD Patients

We previously reported that GPR4 expression was significantly higher in CD patients compared with healthy controls.²³ These results suggested that GPR4 may play a role during inflammation. In the novel work presented here, we sought to elucidate the pathophysiological relevance of pH-sensing GPR4 in fibrosis and to determine its expression in 2 different types of CD patient samples from Netherland residents: (1) fibrotic vs (2) nonfibrotic terminal ileum (Supplementary Table 1). Paired samples for type 1 and 2 were obtained from the thickened fibrosis-affected region and nonfibrosis affected resection margin, respectively, from patients with CD undergoing ileocecal resection due to stenosis in the terminal ileum. G protein-coupled receptor 4 mRNA was significantly increased in fibrosis-affected terminal ileum (Fig. 1A).

Hallmarks of intestinal fibrosis are conformational changes in the cytoskeleton of activated myofibroblasts and the production of extracellular matrix (ECM) proteins. A key marker of myofibroblasts is alpha smooth muscle actin (*ACTA2*), and collagen synthesis is promoted by myofibroblasts.³² In our earlier work, we observed a significant increase in mRNA expression of fibrosis markers *ACTA2*, procollagen type 1 alpha 1 (*COL1A1*), and procollagen type 3 alpha 1 (*COL3A1*) in fibrosis-affected region compared with nonfibrosis-affected resection margin.³³ In the novel work presented here, we also established a significant increase in mRNA expression in the fibrotic intestine in CD patients for *COL1A2* (8.4 ± 8.1 vs 178.8 ± 344.9 ; $n = 8$ each; $*P < 0.05$, Supplementary Fig. 1), connective tissue growth factor (*CTGF*, 14.9 ± 9.3 vs 124.2 ± 171.1 ; $n = 8$ each; $**P < 0.01$), which together with TGF- β perpetuates fibrosis^{32, 34} and vimentin (*VIM*, 4.6 ± 4.6 vs 128.2 ± 298.9 ; $n = 8$ each; $**P < 0.01$), a major structural component of intermediate filaments in fibroblasts.³⁵ A positive linear correlation between GPR4 and *ACTA2* (R 0.871; $***P < 0.001$), *COL1A1* (R 0.915; $***P < 0.001$), *COL1A2* (R 0.506; $*P < 0.05$), *COL3A1* (R 0.915; $***P < 0.001$), *CTGF* (R 0.565; $*P < 0.05$), and *VIM* (R 0.888; $***P < 0.001$) was found (Fig. 1B). This is in line with our hypothesis that the expression of *GPR4* is associated with fibrogenesis.

Low oxygenation—hypoxia—is a central feature of IBD³⁶ and leads to a decrease in pH and an increase in hypoxia inducible factor (*HIF*)1 α mRNA expression. Hypoxia inducible factor 1 α mRNA was significantly increased in fibrosis-affected terminal ileum (Fig. 1C). Hypoxia also enhances induction of intercellular adhesion molecule 1 (*ICAM1*).³⁷ Accordingly, *ICAM1* mRNA was significantly increased in fibrosis-affected terminal ileum (Fig. 1C). In contrast, antimicrobial peptide genes that are known to be reduced in stricturing CD patients,³⁸ defensins *DEFA5* and *DEFA6*, were significantly decreased (Fig. 1C), suggesting a diminished host defense.

In previous, already published work, we confirmed that unaffected resection margins were free of fibrosis; we showed this by comparing these samples with noncancer-affected terminal ileum resection margins from resections due to adenocarcinoma.³³ Furthermore, no differences were observed in mRNA expression levels of *COL1A1*, *COL3A1*, *ACTA2*, and *TGFB1* when comparing fibrosis-affected terminal ileum and unaffected resection margin.³³

To narrow down on which cells of the intestinal mucosa GPR4 are expressed, GPR4 mRNA was quantified in mucosa and crypt samples (Swiss IBD cohort); nonfibrotic mucosal samples were analyzed as non-IBD (Supplementary Table 2). Expression of *GPR4* was higher in whole mucosal tissue compared with isolated crypts (80.3 ± 90.1 ; $n = 13$ vs 7.0 ± 15.1 ; $n = 8$, Fig. 1D). These results suggest that GPR4 is mainly expressed in nonepithelial cells of the lamina propria, such as endothelial cells or fibroblasts.

Fibrosis Is Decreased in *Gpr4*-deficient Mice in DSS-induced Chronic Colitis

In previous work, we assessed the relevance of GPR4 in the development of intestinal inflammation in the DSS mouse model of colitis.²³ The DSS-induced chronic colitis model is one of the most reproducible models driven by chemical injuries in the colonic epithelium. Chronic colitis and fibrosis occur in the final phase of the animal experiment. In our previous study, a total of 22 DSS-treated WT mice and 18 DSS-treated *Gpr4*^{-/-} littermates were compared with 5 WT and 6 *Gpr4*^{-/-} littermates receiving DSS-free water. DSS-treated *Gpr4*^{-/-} mice showed less severe inflammation, less reduction in body weight, and a significantly lower histological score.²³ In the novel work presented here, we reused samples generated from that previous study.²³ To assess the development of fibrosis in the DSS colitis model, we directly evaluated fibrogenesis parameters in *Gpr4*-deficient mice compared with WT mice. mRNA expression of procollagen type 1 alpha 1 (*Col1a1*) was significantly decreased in the colon of *Gpr4*^{-/-} mice compared with WT mice upon DSS treatment (Fig. 2A). mRNA expression of *Acta2*, *Col1a2*, *Col3a1* and *Col16a1* was significantly decreased in the colon of *Gpr4*^{-/-} mice compared with WT mice upon DSS treatment (Fig. 2A). In addition, elastin (*Eln*), a molecular component of ECM expressed by myofibroblasts,³⁹ *Fkbp10*, a collagen 1 chaperone⁴⁰ mainly expressed by myofibroblasts eg in experimental lung fibrosis⁴¹ and regulator of collagen biosynthesis,⁴² and hyaluronan synthase (*Has2*), essential to TGF- β -induced myofibroblast differentiation⁴³ and relevant for the promotion of fibrosis,⁴⁴ were significantly decreased in the colon of *Gpr4*^{-/-} mice (Fig. 2B, Supplementary Fig. 2A). Additionally, 4-Hydroxyproline (HYP), a major component of collagen that can be used as an indicator of collagen content, was reduced (Supplementary Fig. 2B), and the thickness of the collagen layer and collagen content were significantly decreased in *Gpr4*^{-/-} mice (Fig. 2C and D, Supplementary Fig. 2C). In agreement, protein levels of *COL1A1* (1.00 ± 0.39 vs 0.51 ± 0.33), *VIM* (1.00 ± 0.92 vs 0.25 ± 0.23), and TGF β 1 (1.00 ± 0.52 vs 0.52 ± 0.23) were significantly decreased in *Gpr4*^{-/-} mice (Fig. 2E), indicating less severe profibrotic responses.

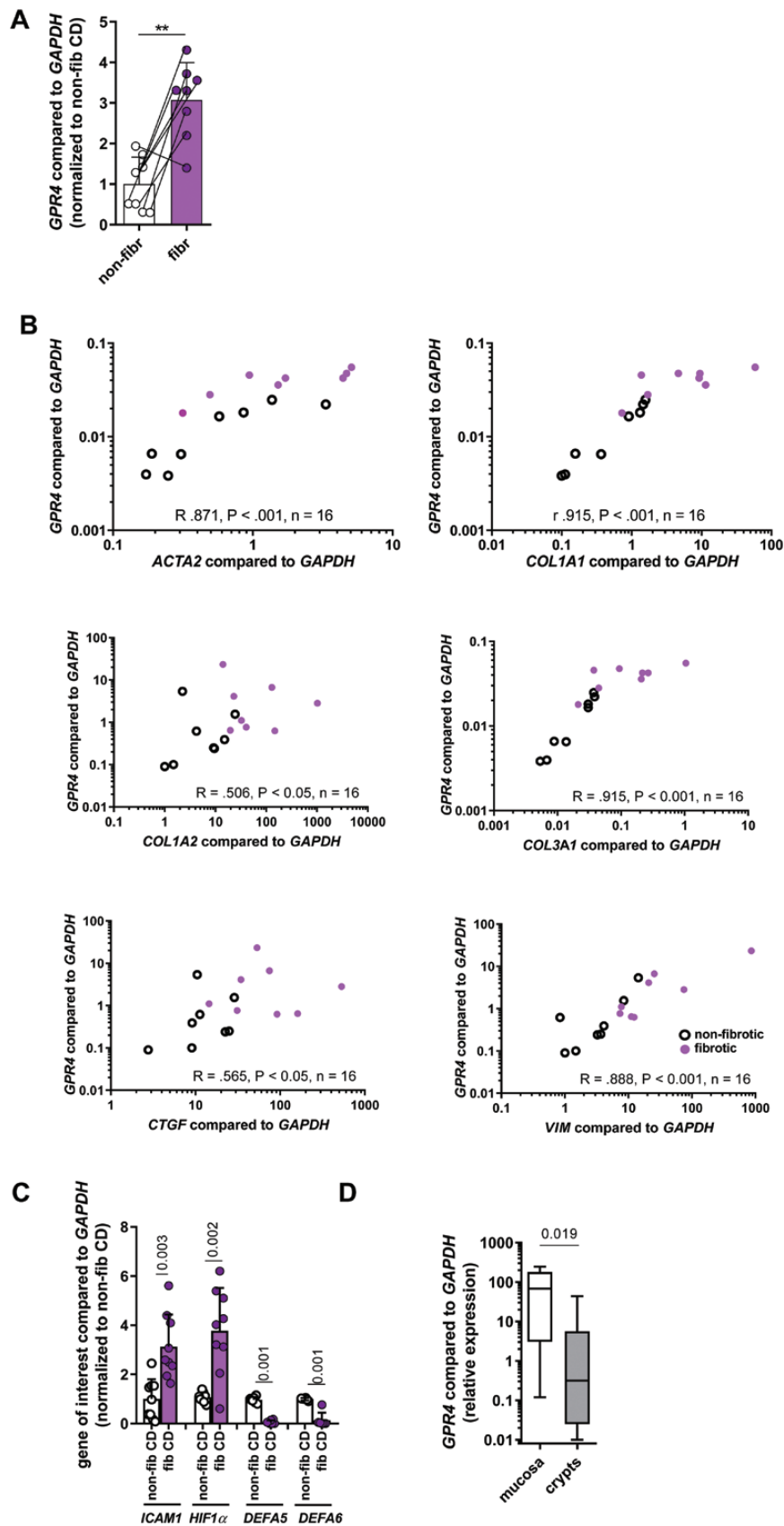


Figure 1. Expression of GPR4 is increased in the fibrotic intestine in CD patients. A, *GPR4* mRNA expression in fibrotic (purple) vs nonfibrotic (white) terminal ileum of patients with CD (16 paired samples from 8 patients, paired *t* test). B, Positive correlation in mRNA expression between *GPR4* vs *ACTA2*, *COL1A1*, *COL1A2*, *COL3A1*, *CTGF*, and *VIM* (Spearman's rank correlation coefficient, 16 samples from 8 nonfibrotic [white] and 8 fibrotic [purple] tissues). C, *ICAM1*, *HIF1 α* , *DEFA5*, and *DEFA6* mRNA expression in fibrotic vs nonfibrotic terminal ileum (paired *t* test from 8, 8, 6, and 7 patients, respectively). D, *GPR4* mRNA expression in mucosa and crypts (unpaired *t* test, Mann-Whitney).

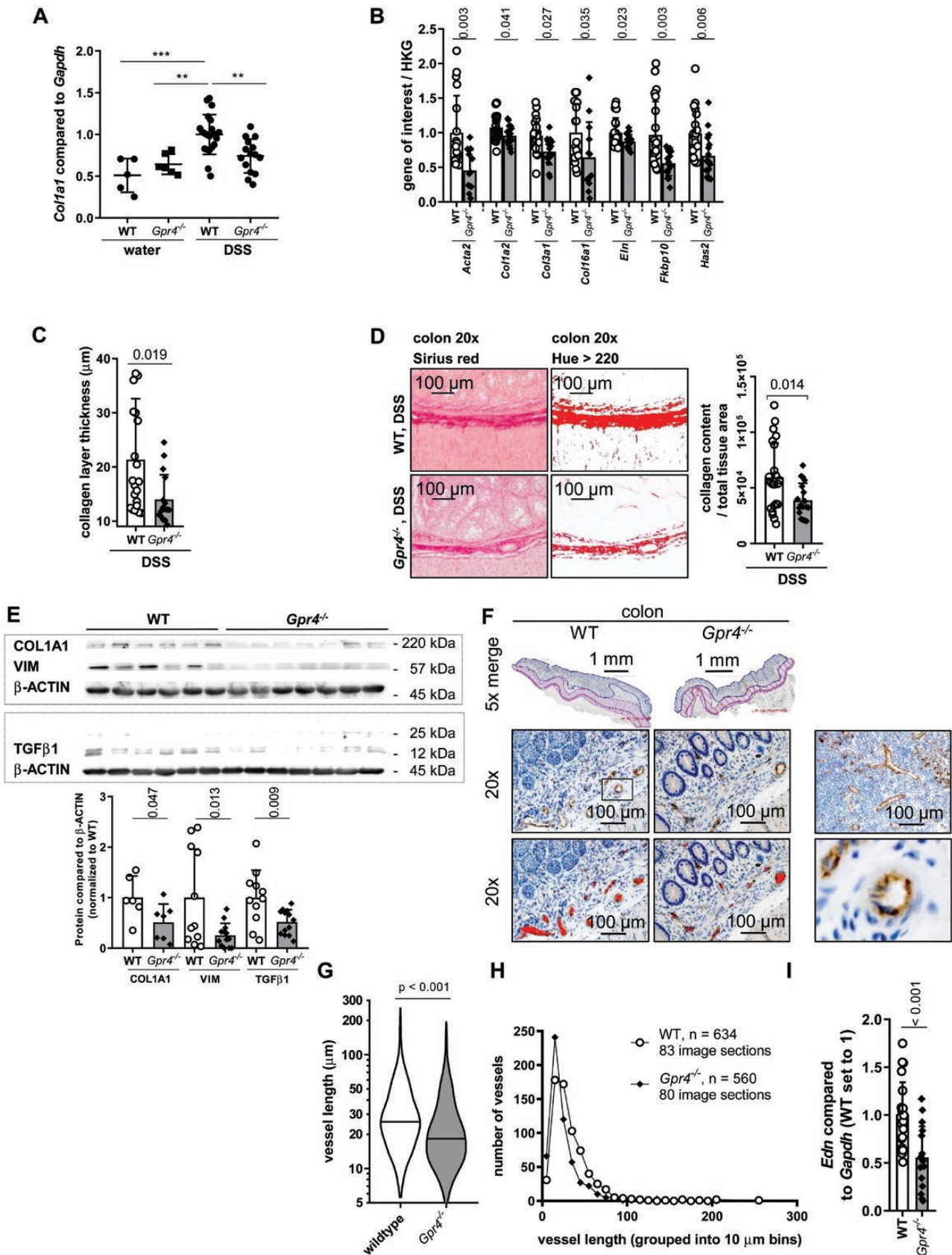


Figure 2. Lack of GPR4 reduces collagen deposition and vessel numbers in the chronic DSS model of inflammation. A, mRNA expression of *Col1a1* ($n = 5, 6, 21,$ and $15,$ ANOVA Tukey's test). B, mRNA expression of profibrotic genes ($n = 13-22,$ unpaired t tests). (C and D) Sirius red staining for collagen layer thickness ($n = 16-22$) and collagen content in 20x images (Fiji; $n = 18-22,$ unpaired t tests). E, COL1A1, VIM, and TGF β 1 WB and densitometry ($n = 6-13,$ unpaired t tests). F, CD31 $^+$ (brown) in colon mucosa (circled in blue). Muscle tissue was excluded (circled in pink). Vessel area highlighted in red. Positive control from spleen. G, Vessel length counted in mucosa. Average length of vascular structures (unpaired t test, median shown). H, Size distribution of vessel lengths grouped into 10 μ m bins (n as indicated). I, *Edn* mRNA expression ($n = 16-21,$ unpaired t tests).

Gpr4 Deficiency Reduces Vascularization in DSS-induced Chronic Colitis

G protein-coupled receptor 4 is strongly expressed in endothelial cells^{20,45} and regulates vascular permeability and endothelial cell responses to VEGF, a growth factor linked to fibrosis development in several tissues.^{20,21,46,47} Consequently, we set out to determine the relevance of GPR4 for vascular status in murine tissue from the DSS model of chronic colitis. Staining of colonic sections for the panendothelial marker CD31 (Fig. 2F) revealed a significant decrease in vessel length in the colon mucosa from *Gpr4*^{-/-} mice compared with WT littermates (Fig. 2G; 32.7 ± 25.8 μm vs 24.3 ± 20.3 μm; mean ± SD). Of note, continuous structures larger than 100 μm in length were more frequent in WT mice compared with *Gpr4*^{-/-} mice in virtually identical areas (Fig. 2H, a total of 634 vessels over an area of 8.490 mm² in WT mice vs 560 vessels over 8.629 mm² in *Gpr4*^{-/-} mice were considered). In agreement, mRNA expression level of endothelin (*Edn*), an endothelial-derived vasoconstrictor peptide associated with vascular dysfunction,⁴⁶ was significantly decreased in *Gpr4*^{-/-} mice (Fig. 2I). Additionally, mRNA expression levels of *Pdgfrβ*, a potent chemoattractant for fibroblasts and other cells,⁴⁸ was reduced in *Gpr4*^{-/-} mice (Supplementary Fig. 2D).

Fibrosis and Vascularization Are Decreased in *Gpr4*-deficient Mice in Spontaneous Colitis

The model of spontaneous colitis in *Il10*-deficient mice is driven by the absence of a well-defined immunoregulatory and anti-inflammatory activity which is otherwise provided by *Il10*. The colon and, less commonly, the small bowel are affected by inflammation and consequently fibrosis. In a previous study by Wang et al,²³ we had also assessed the importance of *Gpr4* in the development of spontaneous colitis in *Il10*-deficient mice. Interleukin-10^{-/-} animals were compared with *Il10*^{-/-} *Gpr4*^{-/-} mice (n = 9 and 16, respectively) at 80 days of age.²³ Interleukin-10^{-/-} *Gpr4*^{-/-} mice showed a significantly decreased histological score and reduced expression levels of pro-inflammatory cytokines and number of CD4⁺ helper cells compared with *Il10*^{-/-} mice.²³ In the present study, we reused the samples generated from this previous study on the spontaneous colitis model to more closely examine the role of GPR4 in the development of fibrosis. *Col3a1* and *Ctgf* mRNA expression was significantly decreased in *Il10*^{-/-} *Gpr4*^{-/-} mice (Fig. 3A). In these mice, *Vim*, *Tgf*, and fibronectin (*Fn*)1, a component of the ECM, mRNA expression was also lower (Supplementary Fig. 3). Collagen layer thickness was significantly reduced in *Il10*^{-/-} *Gpr4*^{-/-} mice compared with *Il10*^{-/-} mice (Fig. 3B), indicating less severe fibrosis.

As for the DSS model, we carried out CD31 staining and determined vessel number and length. Interleukin-10^{-/-} mice were compared with *Il10*^{-/-} *Gpr4*^{-/-} mice (n = 3 and 4, respectively) at 200 days of age. Sections from *Il10*^{-/-} *Gpr4*^{-/-} mice stained for CD31 (Fig. 3C) showed a significantly decreased vessel length compared with *Il10*^{-/-} mice (Fig. 3D, 34.8 ± 24.8 μm vs 30.0 ± 18.0 μm, mean ± SD). Continuous structures larger than 100 μm in length were more frequent in WT mice compared with *Gpr4*^{-/-} mice in virtually identical areas (a total of 472 vessels over an area of 7.979 mm² in *Il10*^{-/-} mice vs 363 vessels over 7.076 mm² in *Il10*^{-/-} *Gpr4*^{-/-} mice were considered; Fig. 3E).

Fibrosis Is Decreased in *Gpr4*-deficient Mice in a Transplantation Model of Intestinal Fibrosis

To confirm and extend results obtained with the DSS and *Il10*^{-/-} spontaneous colitis models, we performed the heterotopic transplantation model to assess fibrosis. Two independent experiments were carried out with 8 WT mice compared with 8 *GPR4*^{-/-} littermates. Body weight remained unchanged in both recipient groups. *Col1a1* and *Col1a2* mRNA expression was significantly decreased in terminal ileum grafts from *Gpr4*^{-/-} mice compared with WT mice (Fig. 4A). The mRNA expression of *Col5a1* (procollagen type 5 alpha 1), *Col12a1* (procollagen type X7 alpha 1), *Has*, and *Eln* mRNA was also lower (Supplementary Fig. 4A). Additionally, collagen content, layer thickness, and HYP levels were significantly decreased in *Gpr4*^{-/-} mice (Fig. 4B and C, Supplementary Fig. 4B), indicating less severe profibrotic responses.

The GPR4 Antagonist Decreases Collagen Deposition in Mice

We used the same model to assess the effect of the GPR4 antagonist 39c on fibrogenesis. The GPR4 antagonist was applied IP in a dose-dependent manner 3 times daily for 7 days starting on the day of transplantation. The mRNA expression of *Col12a1* decreased in grafts from mice treated with the antagonist (30 mg per kg mouse weight, 3 times daily), compared with vehicle (Fig. 5A). *Col3a1* was lower in grafts from mice treated with antagonist (Supplementary Fig. 5). The 4-Hydroxyproline (Fig. 5B) and collagen content (Fig. 5C) were significantly decreased in a dose-dependent manner, indicating less severe fibrosis. The GPR4 antagonist 39c further corroborates results from *Gpr4*^{-/-} mice in murine models of intestinal fibrosis, indicating that collagen deposition is reduced in the absence of GPR4 signaling.

In the heterotopic transplantation model, mRNA expression of *Vegfa* was significantly decreased in the presence of the GPR4 antagonist in a dose-dependent manner (Fig. 5D). The presence of shorter vessels and decreased angiogenic factors was indicative of less vascularisation in all 3 models.

Evidence for GPR4 Expression in Intestinal Fibroblasts

To localize and characterize GPR4 expression in the mouse colon, we employed a reporter knock-in mouse model.²⁷ In brief, mice in which CRE was knocked into the GPR4 locus were crossed with a ROSA-EGFP-reporter line to activate the dormant EGFP expression cassette (Supplementary Fig. 6A). As expected, GFP, indicative of GPR4, was expressed in endothelial cells (Supplementary Fig. 6B) and F4/80⁺ macrophages (Supplementary Fig. 6C). In addition, a GFP signal is found in ACTA2⁺ fibroblasts in mice upon DSS-induced acute colitis (Fig. 6A and B). The ACTA2⁺ fibroblasts were shown to be negative for endothelial cell marker CD31 and F4/80 (Supplementary Fig. 7 and 8). Next, we determined *Gpr4* mRNA levels in intestinal fibroblasts. The qPCR analysis confirmed that *Gpr4* is expressed in primary intestinal fibroblasts isolated and cultured from WT mice but not from *Gpr4*^{-/-} mice (Fig. 6C). After an acidic pH shift for 24 hours, qPCR analysis revealed an increase of *Gpr4* mRNA levels in murine and human fibroblasts (Supplementary Fig. 9A).

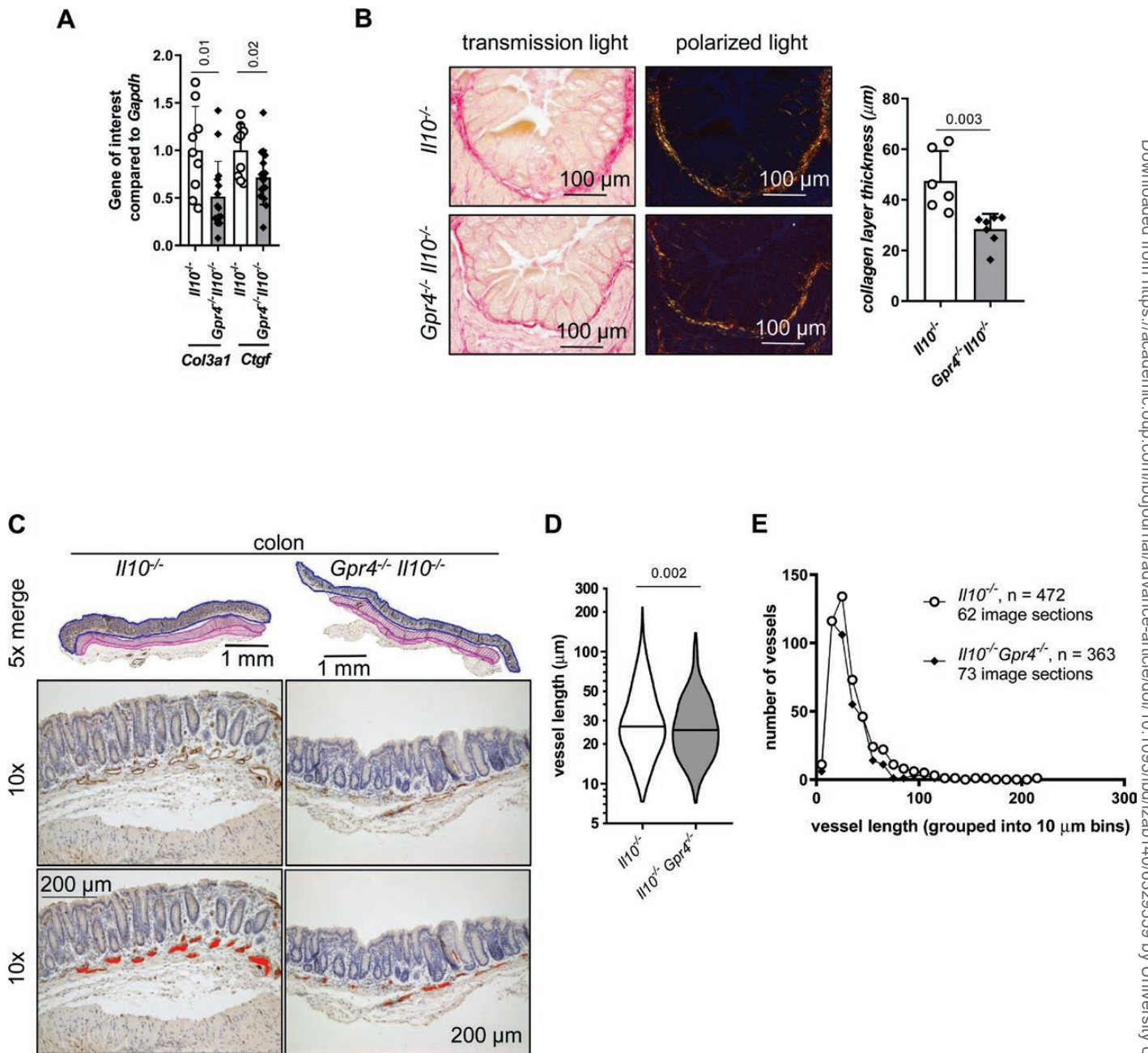


Figure 3. Lack of GPR4 reduces collagen deposition in the spontaneous model of inflammation. A, mRNA expression of profibrotic genes (unpaired *t* test; *n* = 9–13). B, Sirius red staining, collagen layer thickness (Fiji, unpaired *t* test; *n* = 6–7). C, CD31⁺ vessels. D, Vessel length (unpaired *t* test, median shown). E, Size distribution (*n* as indicated).

Activation of Mesenchymal Cells Initiated by Low pH is Prevented by GPR4 Inhibition

To elucidate the pathophysiological relevance of the presence of GPR4 in intestinal fibroblasts, we investigated the effects of GPR4 inhibition in cultured primary murine intestinal fibroblasts. After an acidic pH shift for 24 hours, qPCR analysis revealed an increase of *Acta2*, *Col3a1*, *Ctgf*, *Fn*, and *Vim* mRNA levels, which was reversed in the presence of the GPR4 antagonist 39c (Fig. 6D).

In primary human fibroblasts, IF revealed an increased *ACTA2* expression at low pH, indicating fibroblast-to-myofibroblast transition. The *ACTA2* mRNA expression was reversed in the presence of the GPR4 antagonist (Fig. 7A). An acidic pH-shift significantly increased *ACTA2* protein levels

in primary human fibroblasts (Fig. 7B), and the GPR4 antagonist significantly decreased *ACTA2* expression.

Next, we sought to determine the related signaling pathway. The GPR4 signals via G_{12/13} through guanosine triphosphate-Ras homologous A (GTP-RhoA). The RhoA activity significantly increased after an acidic pH-shift in human fibroblasts, which decreased upon treatment with the GPR4 antagonist (Supplementary Fig. 9B). Phalloidin staining revealed an increased formation of actin stress fibers at pH 6.8 when compared with pH 7.8 (Fig. 7C). Stress fiber formation was reduced upon treatment with the GPR4 antagonist. Our results indicate a pH-dependent GPR4-mediated activation of RhoA and polymerization of actin fibers.

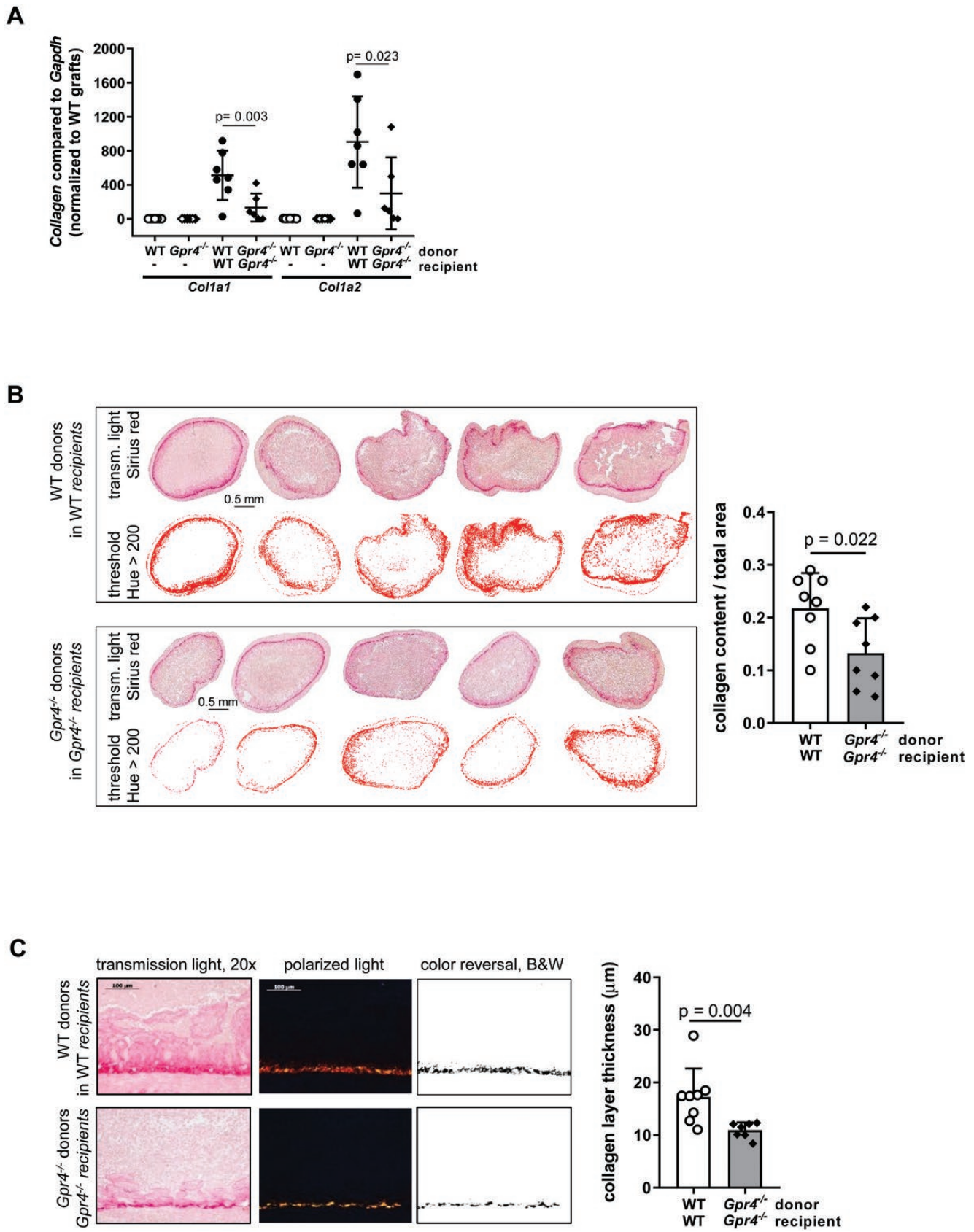


Figure 4. GPR4 antagonist reduces deposition of collagen in the heterotopic transplantation model. A, *Col1a1* and *Col1a2* mRNA expression (ANOVA Tukey's test; n = 6–7). B, Collagen content visualized by Sirius red staining was quantified with the Fiji software (unpaired *t* tests; n = 8 each). C, Collagen layer thickness visualized under polarizing light and measured with the software ZEN (Zeiss, unpaired *t* tests, Mann-Whitney; n = 7–8).

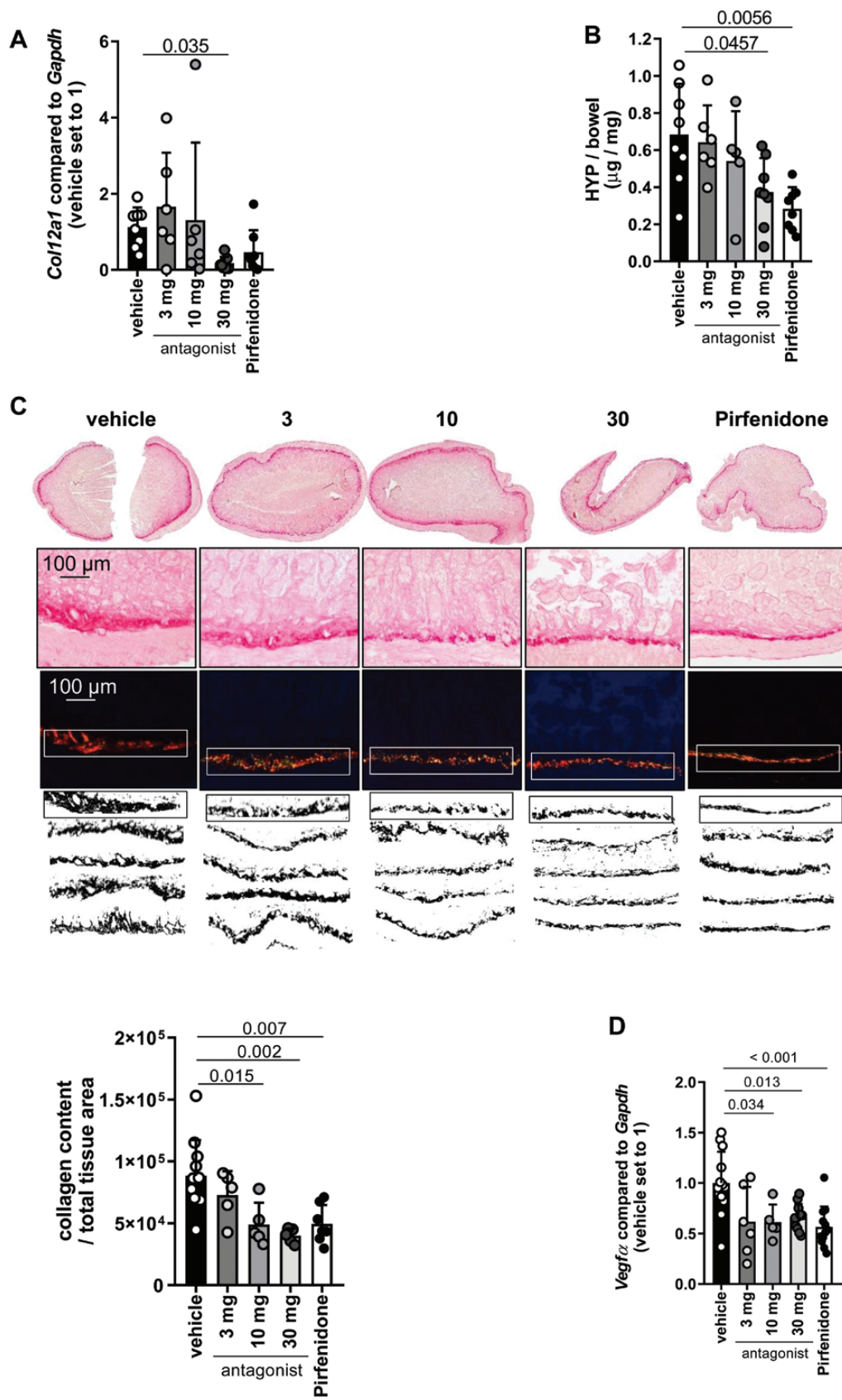


Figure 5. GPR4 antagonist reduces collagen deposition in the heterotopic transplantation model. A, *Col12a1* mRNA expression (ANOVA, Dunn's multiple comparison test; n = 6–8). B, HYP assay (ANOVA Tukey's test; n = 5–8). C, Collagen layer thickness visualized by Sirius red staining was quantified under polarizing light, collagen content (Fiji, ANOVA Tukey's test; n = 5–10). D, *Vegfr2* mRNA expression in the model of heterotopic transplantation (ANOVA Tukey's test; n = 5–12).

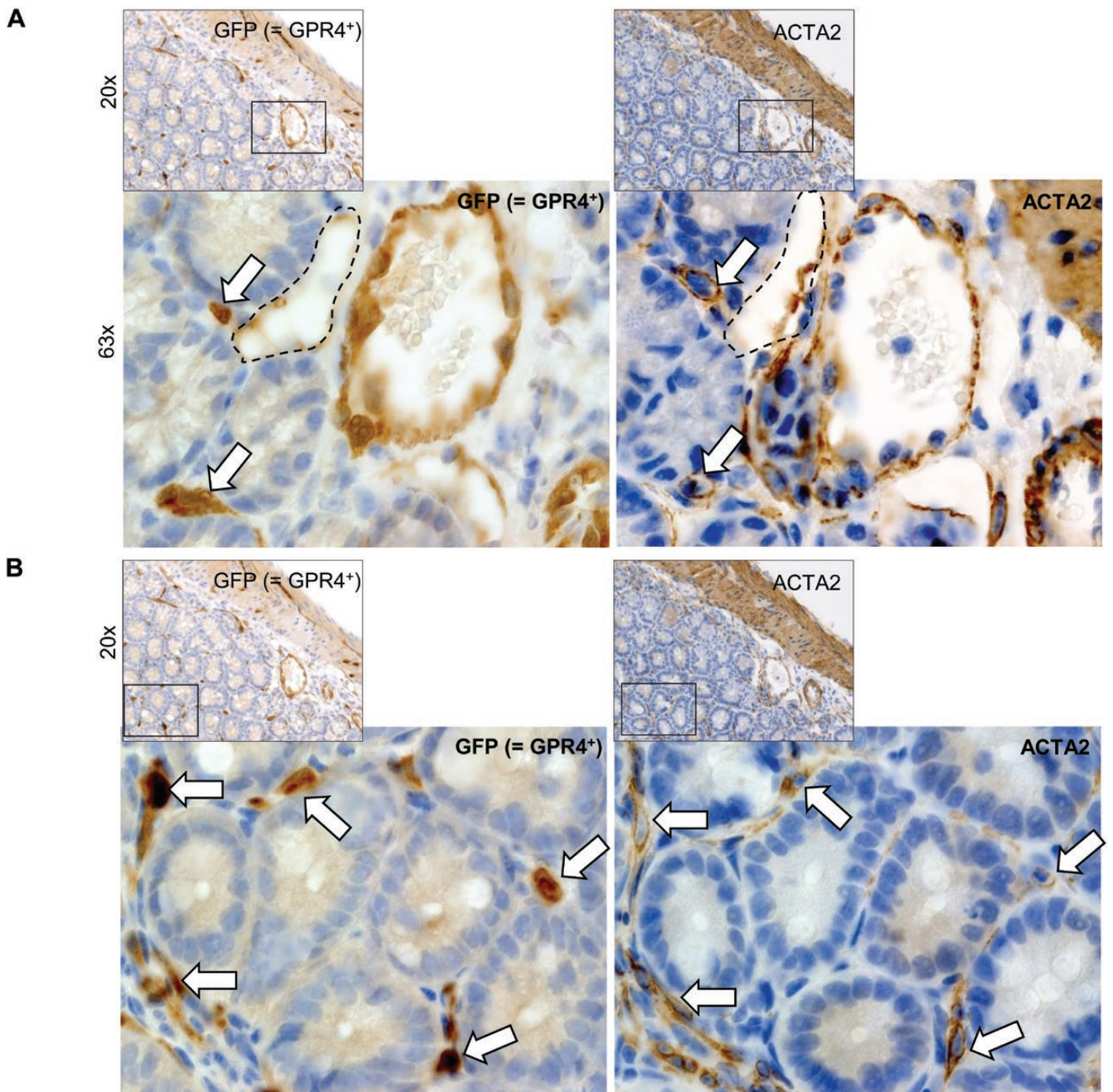


Figure 6. Evidence for GPR4 expression in murine fibroblasts. GPR4 inhibition abrogates fibroblast activation. A–B, Cross sections of terminal ileum obtained from *Gpr4Cre^{+/+} × R26pCAGeGFP^{+/+}* reporter mice at the age of 10 weeks upon DSS-induced acute colitis. Left panel GFP, indicative of GPR4 expression, right panel ACTA2. Arrows point to *ACTA2*⁺ fibroblasts, distant from blood vessels, that appear also positive for GFP. Brown = DAB; original magnification 20x and 63x, respectively. C, *Gpr4* mRNA expression in primary murine fibroblasts isolated from WT mice as assessed by qPCR; n = 3 technical replicates. D, GPR4 inhibitor decreased *Acta2*, *Col3a1*, *Ctgf*, *Fn* and *Vim* mRNA expression (n = as indicated, different fibroblast lines, ANOVA, Tukey's test).

Discussion

In the present study, we investigated the role of the pH-sensing receptor GPR4 in the development of fibrosis. When analyzing the paired samples of the terminal ileum from patients with CD, we observed an increased expression of *GPR4* in the fibrosis-affected area compared with the nonfibrotic resection margin. We also found a positive correlation between

GPR4 and the expression of markers involved in different phases of fibrosis (eg, *ACTA2*, a marker for myofibroblast activation, or the procollagens *COL1A1* and *COL3A1*). Using well-established in vivo murine models for intestinal fibrosis, we demonstrated that *Gpr4* deficiency led to a significant decrease in the transcriptional expression of fibrosis markers and a decrease in collagen layer thickness and HYP compared

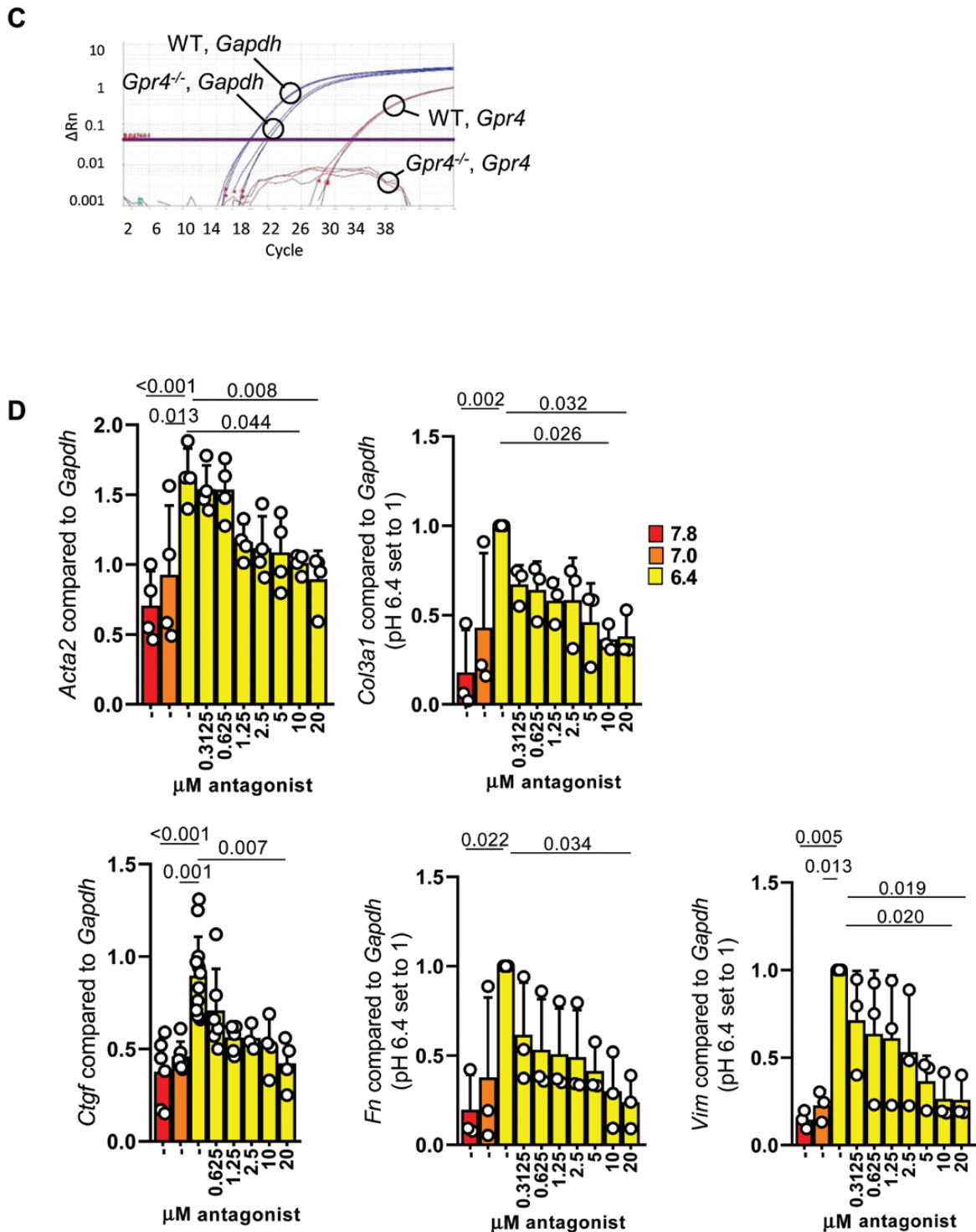


Figure 6. Continued.

with WT mice. In response to DSS-induced colitis, *Gpr4*^{-/-} mice also showed decreased levels of IL-1 β , suggesting a role for GPR4 in driving intestinal inflammation. Inflammasome activation and the resulting high levels of IL-1 β have been associated in the past with active colitis lesions and indicate tissue damage.

These results are in line with earlier work, where inhibition of the pH-sensing receptor GPR4, which shows strong expression in endothelial cells, was shown to exert anti-inflam-

matory, anti-angiogenic, and analgesic actions.^{20, 25, 49} Indeed, our results showed that deficiency of *Gpr4* is associated with a decrease in angiogenesis and decreased expression of *Pdgfr β* and *Vegfa*, which are relevant factors involved in this process. In CD, chronic inflammation is clearly associated with angiogenesis and with increased *VEGF* and bFGF (basic fibroblast growth factor) levels.^{18, 19, 50} G-protein coupled receptor 4 regulates vascular permeability and endothelial cell responses to VEGF. Additionally, VEGF signaling has been

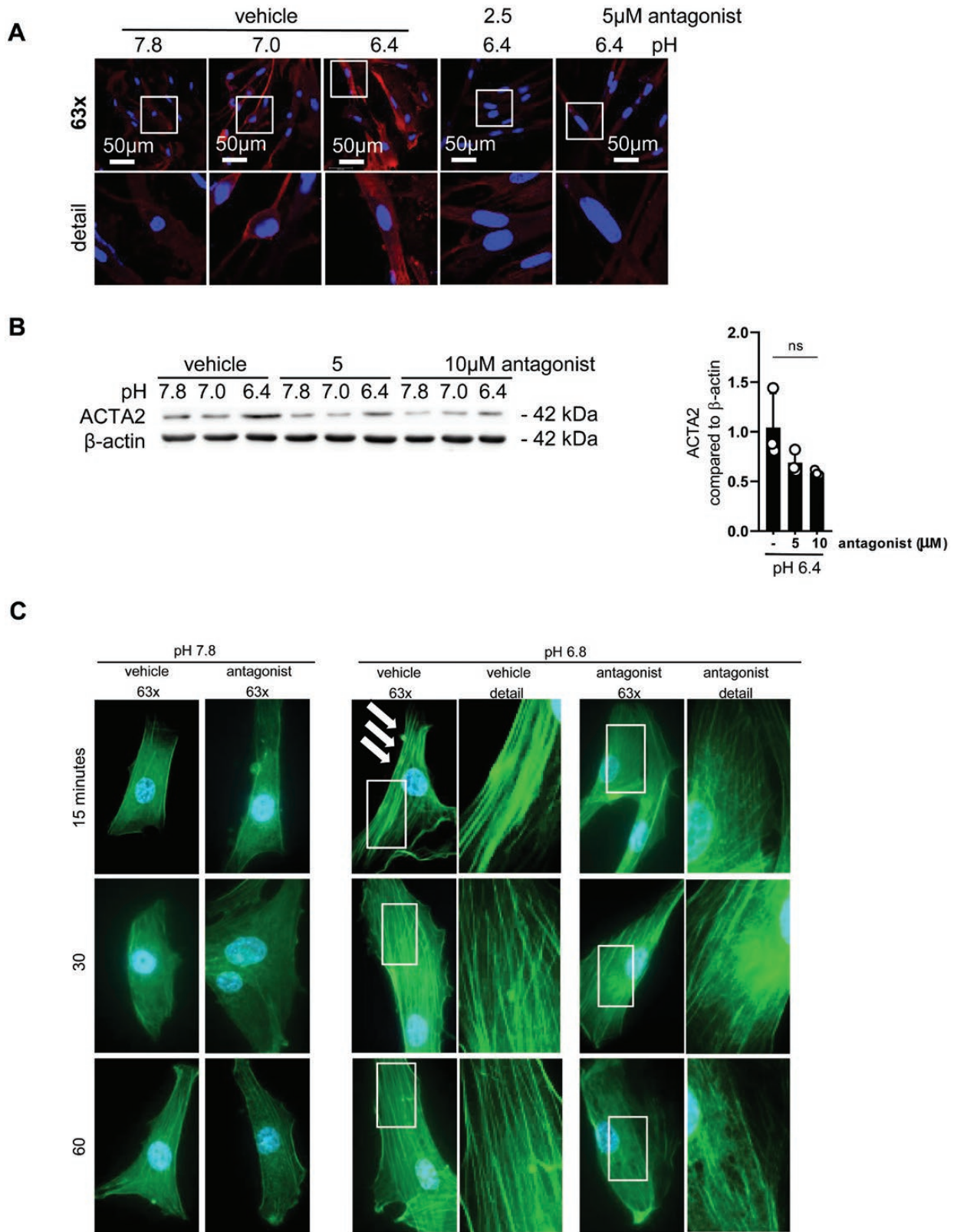


Figure 7. Low pH increases stress fibers in intestinal fibroblasts. GPR4 inhibition abrogates fibroblast activation. Human fibroblasts. A, Immunofluorescence (IF), GPR4 inhibitor decreased ACTA2. Fibroblasts were stimulated for 24 hours. IF for red = ACTA2, and blue = DAPI. Representative image for n = 2. B, WB for ACTA2, ANOVA, Tukey's test, 3 different human fibroblast lines. C, Fluorescent staining with and without antagonist 10 μ M, phalloidin (green), stress fibers (arrows), DAPI (blue), original magnification 63x.

shown to stimulate myofibroblast transformation through the induction of TGF β 1,^{21,22} a powerful profibrotic mediator upregulated in IBD. Mice deficient in *Gpr4* mice show a reduced angiogenic response to VEGF,²⁰ which indicates that sensing tissue acidosis through GPR4 by endothelial cells is required for VEGF action. The interplay between GPR4 and VEGF suggests a form of “co-incidence detection” of acidosis and hypoxia in challenged tissue. The exact mechanism of interaction is not yet known. Nonetheless, available data suggest that it may involve GPR4 signal transduction through $G\alpha_{12/13}$ /RhoA and inhibition of VEGFR2 expression in endothelial cells.⁵¹ In agreement with the data obtained with *Gpr4*-deficient mice, the GPR4 antagonist compound 39c led to reduced *Vegfa* expression and collagen deposition in intestinal tissue in vivo.

G-protein coupled receptor 4 expression has been reported in rat kidney fibroblasts,⁵² and in this study, we confirmed GPR4 expression in intestinal fibroblasts. Baseline levels of GPR4 may already be sufficient to promote inflammation or fibrosis. Interestingly, we determined increased GPR4 levels after an acidic pH shift. Elevated numbers of GPR4⁺ myofibroblasts in intestinal fibrosis may arise by increased migration, proliferation, and differentiation of fibroblasts and through transition from endothelial cells and pericytes. Evidence has recently emerged indicating that fibrosis can also result from mechanisms involving previously unknown transition and cell differentiation.⁵³ Endothelial-to-mesenchymal transition (EndoMT) is known to be driven by inflammation⁵⁴ and could contribute to an increased number of GPR4⁺ mesenchymal cells. Tissue growth factor β 1 plays a central role as an inducer of EndoMT.^{55,56} Endothelial-to-mesenchymal transition can also occur under the influence of chronic inflammatory stimuli.⁵⁷ In experimental cardiac fibrosis, TGF- β 1 also mediates EndoMT. Interestingly, the preservation of the endothelial phenotype by rhBMP-7 is followed by a reduction of EndoMT and correlates to inhibition of fibrosis.⁵⁵ The GPR4⁺ pericytes²⁴ surrounding the vascular system also represent a cellular reservoir for fibroblasts during tissue repair⁵⁸ that can detach from vessels for transition into COL1A-producing fibroblast in experimental dermal scarring.⁵⁹ We hypothesize that GPR4⁺ fibroblasts originate at least in part from endothelial cells and pericytes.

The model of DSS-induced chronic colitis has its own limitations with regard to the development of intestinal fibrosis.⁶⁰ In this model, chronic colitis is initiated by chemical injury; nonetheless, there is no evidence that IBD is initiated by chemical injury in the intestinal mucosa. In spite of this, injury can be useful to study epithelial inflammation and subepithelial fibrosis in UC.⁶⁰ The model of spontaneous colitis has its own limitations, as well. In this model, the occurrence and severity of inflammation and fibrosis greatly depends on the breeding facility,⁶⁰ most likely on hygiene levels, and gut microbiota composition.

Our in vitro assays with primary human and murine intestinal fibroblasts showed that acidic pH initiated myofibroblast activation, evidenced by an increase in the expression of corresponding markers (*ACTA2* and *Ctgf*). The GPR4 signaling occurs via $G\alpha_{12/13}$ through activation of GTP-RhoA and Rho kinase (ROCK). Rho kinase triggers subsequent actin polymerization and stress fiber formation, thereby impacting cell shape and cytoskeletal integrity. Rho kinase inhibition was proposed as a treatment for fibrosis in neovascular age-related

macular degeneration,⁶¹ pulmonary fibrosis,⁶² and intestinal fibrosis. In the present study, GTP-RhoA was increased upon acidic pH treatment in fibroblasts, suggesting a dominant signalling through $G\alpha_{12/13}$ in the present context. Activated RhoA and GTP-RhoA-mediated stress fiber formation were decreased in the presence of the GPR4 antagonist, supporting the notion of pH-mediated GPR4/ $G\alpha_{12/13}$ signaling in fibroblasts.

Conclusion

Our results show that *GPR4* expression correlates positively with the expression of profibrotic genes and levels of collagen deposition in fibrotic sections from patients with CD compared with nonfibrotic control sections. In murine models of colitis, *Gpr4* deficiency and GPR4 inhibition were associated with decreased fibrogenesis and vascularisation. Some GPR4⁺ fibroblasts may originate from GPR4⁺ endothelial cells and pericytes. A smaller number of blood vessels would also reduce the source of newly emerging myofibroblasts in fibrotic areas. Further research should be directed toward a better understanding of how acidosis, the vascular system, and fibroblasts interact to drive inflammation and fibrosis in CD patients. G-protein coupled receptor 4 present in endothelial cells and fibroblasts represents a potential new target for therapeutic intervention. Further research is needed to assess the impact of the GPR4 inhibitor in CD-derived fibroblasts.

Supplementary data

Supplementary data is available at *Inflammatory Bowel Diseases* online.

Acknowledgments

Authors would like to thank Marie G. Ludwig for support and discussion.

Data Availability

The data underlying this article are available in a repository provided by the University of Zurich [the link to the repository still needs to be defined] with the exception of the patient data underlying this article. Patient data cannot be shared publicly due to the privacy of individuals that participated in the according study.

Author Contribution

MH and GR conceptualized the study. BW, WTVvH curated data and wrote the article. CM, BW, KB, SH, FS, SM, EP, PHIS, FS, and CS curated data. GD, CdV, CAW, IFW, KS, YW, FS, PAR, MH wrote, reviewed, and edited the article. All authors approved the final submitted version of the manuscript.

Supported by

This work was supported by research grants from the Swiss National Science Foundation (grant number 314730_152895/1) and FreeNovation from Novartis to

MH; the Swiss National Science Foundation (grant number 31003A_176125) to CAW; the National Center of Competence in Research NCCR Kidney.CH to PHIS and CAW; the Swiss National Science Foundation (grant numbers 310030_172870, 314730_153380) to GR; the Swiss National Science Foundation (grant numbers 3100 A0 -122114/1, 310030 169196), and the European Research Advisory Board (ERAB; grant number EA 09 20) to FS.

Presented at

Data were presented at the Keystone symposia, February 19–23, 2020, Q5/Q6: Fibrosis and Tissue Repair: From Molecules and Mechanics to Therapeutic Approaches

Conflicts of Interest

MH discloses grant support from AbbVie and Novartis. GD discloses unrestricted grants from Abbvie and Takeda, is on the advisory boards for Mundipharma and Pharmacosmos, and receives speakers fees from Takeda and Janssen pharmaceuticals. WTvH received funding for printing of his PhD thesis from Ferring, Teva, Tramedicos and Mylan. FS discloses grant support and lecture fees from AbbVie and Gilead. MSD, BW, FS, EP, SM, SH, KB, YW, CM, CdV, PHIS, CAW, IFW, and PAR have no conflict of interest to disclose. GR discloses grant support from AbbVie, Ardeypharm, MSD, FALK, Flamentera, Novartis, Roche, Tillots, UCB, and Zeller. All other authors have nothing to disclose.

References

- Fallingborg J, Christensen LA, Jacobsen BA, et al. Very low intraluminal colonic pH in patients with active ulcerative colitis. *Dig Dis Sci*. 1993;38:1989–1993.
- Nugent SG, Kumar D, Rampton DS, et al. Intestinal luminal pH in inflammatory bowel disease: possible determinants and implications for therapy with aminosalicylates and other drugs. *Gut*. 2001;48:571–577.
- Press AG, Hauptmann IA, Hauptmann L, et al. Gastrointestinal pH profiles in patients with inflammatory bowel disease. *Aliment Pharmacol Ther*. 1998;12:673–678.
- Lardner A. The effects of extracellular pH on immune function. *J Leukoc Biol*. 2001;69:522–530.
- Hanly EJ, Aurora AA, Shih SP, et al. Peritoneal acidosis mediates immunoprotection in laparoscopic surgery. *Surgery*. 2007;142:357–364.
- Brokelman WJ, Lensvelt M, Borel Rinke IH, et al. Peritoneal changes due to laparoscopic surgery. *Surg Endosc*. 2011;25:1–9.
- Mogi C, Tobo M, Tomura H, et al. Involvement of proton-sensing TDAG8 in extracellular acidification-induced inhibition of proinflammatory cytokine production in peritoneal macrophages. *J Immunol*. 2009;182:3243–3251.
- de Bruyn JR, Meijer SL, Wildenberg ME, et al. Development of fibrosis in acute and longstanding ulcerative colitis. *J Crohns Colitis*. 2015;9:966–972.
- Cosnes J, Cattan S, Blain A, et al. Long-term evolution of disease behavior of Crohn's disease. *Inflamm Bowel Dis*. 2002;8:244–250.
- Latella G, Papi C. Crucial steps in the natural history of inflammatory bowel disease. *World J Gastroenterol*. 2012;18:3790–3799.
- Rieder F, Fiocchi C. Intestinal fibrosis in IBD—a dynamic, multifactorial process. *Nat Rev Gastroenterol Hepatol*. 2009;6:228–235.
- Matsuzaki S, Ishizuka T, Yamada H, et al. Extracellular acidification induces connective tissue growth factor production through proton-sensing receptor OGR1 in human airway smooth muscle cells. *Biochem Biophys Res Commun*. 2011;413:499–503.
- Kodric M, Shah AN, Fabbri LM, et al. An investigation of airway acidification in asthma using induced sputum: a study of feasibility and correlation. *Am J Respir Crit Care Med*. 2007;175:905–910.
- Seuwen K, Ludwig MG, Wolf RM. Receptors for protons or lipid messengers or both? *J Recept Signal Transduct Res*. 2006;26:599–610.
- Ludwig MG, Vanek M, Guerini D, et al. Proton-sensing G-protein-coupled receptors. *Nature*. 2003;425:93–98.
- Wang JQ, Kon J, Mogi C, et al. TDAG8 is a proton-sensing and psychosine-sensitive G-protein-coupled receptor. *J Biol Chem*. 2004;279:45626–45633.
- Ishii S, Kihara Y, Shimizu T. Identification of T cell death-associated gene 8 (TDAG8) as a novel acid sensing G-protein-coupled receptor. *J Biol Chem*. 2005;280:9083–9087.
- Danese S, Sans M, de la Motte C, et al. Angiogenesis as a novel component of inflammatory bowel disease pathogenesis. *Gastroenterology*. 2006;130:2060–2073.
- Scaldaferri F, Vetrano S, Sans M, et al. VEGF-A links angiogenesis and inflammation in inflammatory bowel disease pathogenesis. *Gastroenterology*. 2009;136:585–95.e5.
- Wyder L, Suply T, Ricoux B, et al. Reduced pathological angiogenesis and tumor growth in mice lacking GPR4, a proton sensing receptor. *Angiogenesis*. 2011;14:533–544.
- Park HY, Kim JH, Park CK. VEGF induces TGF- β 1 expression and myofibroblast transformation after glaucoma surgery. *Am J Pathol*. 2013;182:2147–2154.
- Li ZD, Bork JP, Krueger B, et al. VEGF induces proliferation, migration, and TGF- β 1 expression in mouse glomerular endothelial cells via mitogen-activated protein kinase and phosphatidylinositol 3-kinase. *Biochem Biophys Res Commun*. 2005;334:1049–1060.
- Wang Y, de Vallière C, Imenez Silva PH, et al. The proton-activated receptor GPR4 modulates intestinal inflammation. *J Crohns Colitis*. 2018;12:355–368.
- Martin JC, Chang C, Boschetti G, et al. Single-cell analysis of Crohn's disease lesions identifies a pathogenic cellular module associated with resistance to anti-TNF therapy. *Cell*. 2019;178:1493–1508.e20.
- Miltz W, Velcicky J, Dawson J, et al. Design and synthesis of potent and orally active GPR4 antagonists with modulatory effects on nociception, inflammation, and angiogenesis. *Bioorg Med Chem*. 2017;25:4512–4525.
- Sanderlin EJ, Marie M, Velcicky J, et al. Pharmacological inhibition of GPR4 remediates intestinal inflammation in a mouse colitis model. *Eur J Pharmacol*. 2019;852:218–230.
- Hosford PS, Mosienko V, Kishi K, et al. CNS distribution, signalling properties and central effects of G-protein coupled receptor 4. *Neuropharmacology*. 2018;138:381–392.
- Tchorz JS, Suply T, Ksiazek I, et al. A modified RMCE-compatible Rosa26 locus for the expression of transgenes from exogenous promoters. *Plos One*. 2012;7:e30011.
- Hausmann M, Rechsteiner T, Caj M, et al. A new heterotopic transplant animal model of intestinal fibrosis. *Inflamm Bowel Dis*. 2013. doi: [10.1097/MIB.0b013e3182a6a0f3](https://doi.org/10.1097/MIB.0b013e3182a6a0f3).
- Rittié L. Method for picrosirius red-polarization detection of collagen fibers in tissue sections. *Methods Mol Biol*. 2017;1627:395–407.
- Maeyashiki C, Melhem H, Hering L, et al. Activation of pH-sensing receptor OGR1 (GPR68) induces ER stress via the IRE1 α /JNK pathway in an intestinal epithelial cell model. *Sci Rep*. 2020;10:1438.
- Lawrance IC, Rogler G, Bamias G, et al. Cellular and molecular mediators of intestinal fibrosis. *J Crohns Colitis*. 2017;11:1491–1503.
- Hutter S, van Haaften WT, Hünerwadel A, et al. Intestinal activation of pH-sensing receptor OGR1 [GPR68] contributes to fibrogenesis. *J Crohns Colitis*. 2018;12:1348–1358.
- Mori T, Kawara S, Shinozaki M, et al. Role and interaction of connective tissue growth factor with transforming growth factor-

- beta in persistent fibrosis: a mouse fibrosis model. *J Cell Physiol.* 1999;181:153–159.
35. Wang N, Stamenovic D. Mechanics of vimentin intermediate filaments. *J Muscle Res Cell Motil.* 2002;23:535–540.
36. Manresa MC, Taylor CT. Hypoxia inducible factor (HIF) hydroxylases as regulators of intestinal epithelial barrier function. *Cell Mol Gastroenterol Hepatol.* 2017;3:303–315.
37. Zünd G, Uezono S, Stahl GL, et al. Hypoxia enhances induction of endothelial ICAM-1: role for metabolic acidosis and proteasomes. *Am J Physiol.* 1997;273:C1571–C1580.
38. Wang J, Ortiz C, Fontenot L, et al. High circulating elafin levels are associated with Crohn's disease-associated intestinal strictures. *Plos One.* 2020;15:e0231796.
39. Speca S, Giusti I, Rieder F, et al. Cellular and molecular mechanisms of intestinal fibrosis. *World J Gastroenterol.* 2012;18:3635–3661.
40. Ishikawa Y, Vranka J, Wirz J, et al. The rough endoplasmic reticulum-resident FK506-binding protein FKBP65 is a molecular chaperone that interacts with collagens. *J Biol Chem.* 2008;283:31584–31590.
41. Staab-Weijnitz CA, Fernandez IE, Knüppel L, et al. FK506-binding protein 10, a potential novel drug target for idiopathic pulmonary fibrosis. *Am J Respir Crit Care Med.* 2015;192:455–467.
42. Knüppel L, Heinzelmann K, Lindner M, et al. FK506-binding protein 10 (FKBP10) regulates lung fibroblast migration via collagen VI synthesis. *Respir Res.* 2018;19:67.
43. Webber J, Jenkins RH, Meran S, et al. Modulation of TGFbeta1-dependent myofibroblast differentiation by hyaluronan. *Am J Pathol.* 2009;175:148–160.
44. Li Y, Jiang D, Liang J, et al. Severe lung fibrosis requires an invasive fibroblast phenotype regulated by hyaluronan and CD44. *J Exp Med.* 2011;208:1459–1471.
45. Krewson EA, Sanderlin EJ, Marie MA, et al. The proton-sensing GPR4 receptor regulates paracellular gap formation and permeability of vascular endothelial cells. *Iscience.* 2020;23:100848.
46. Davenport AP, Hyndman KA, Dhaun N, et al. Endothelin. *Pharmacol Rev.* 2016;68:357–418.
47. Zhang J, Chu M. Differential roles of VEGF: relevance to tissue fibrosis. *J Cell Biochem* 2019. doi: [10.1002/jcb.28489](https://doi.org/10.1002/jcb.28489).
48. Roskoski R Jr. The role of small molecule platelet-derived growth factor receptor (PDGFR) inhibitors in the treatment of neoplastic disorders. *Pharmacol Res.* 2018;129:65–83.
49. Dong L, Li Z, Leffler NR, et al. Acidosis activation of the proton-sensing GPR4 receptor stimulates vascular endothelial cell inflammatory responses revealed by transcriptome analysis. *Plos One.* 2013;8:e61991.
50. Alkim C, Alkim H, Koksar AR, et al. Angiogenesis in Inflammatory Bowel Disease. *Int J Inflamm.* 2015;2015:970890.
51. Sivaraj KK, Takefuji M, Schmidt I, et al. G13 controls angiogenesis through regulation of VEGFR-2 expression. *Dev Cell.* 2013;25:427–434.
52. Riemann A, Ihling A, Thomas J, et al. Acidic environment activates inflammatory programs in fibroblasts via a cAMP-MAPK pathway. *Biochim Biophys Acta.* 2015;1853:299–307.
53. Rieder F, Fiocchi C. Intestinal fibrosis in inflammatory bowel disease—current knowledge and future perspectives. *J Crohns Colitis.* 2008;2:279–290.
54. Rieder F, Kessler SP, West GA, et al. Inflammation-induced endothelial-to-mesenchymal transition: a novel mechanism of intestinal fibrosis. *Am J Pathol.* 2011;179:2660–2673.
55. Zeisberg EM, Tarnavski O, Zeisberg M, et al. Endothelial-to-mesenchymal transition contributes to cardiac fibrosis. *Nat Med.* 2007;13:952–961.
56. Arciniegas E, Sutton AB, Allen TD, et al. Transforming growth factor beta 1 promotes the differentiation of endothelial cells into smooth muscle-like cells in vitro. *J Cell Sci.* 1992;103 (Pt 2):521–529.
57. Chaudhuri V, Zhou L, Karasek M. Inflammatory cytokines induce the transformation of human dermal microvascular endothelial cells into myofibroblasts: a potential role in skin fibrogenesis. *J Cutan Pathol.* 2007;34:146–153.
58. Gerhardt H, Betsholtz C. Endothelial-pericyte interactions in angiogenesis. *Cell Tissue Res.* 2003;314:15–23.
59. Sundberg C, Ivarsson M, Gerdin B, et al. Pericytes as collagen-producing cells in excessive dermal scarring. *Lab Invest.* 1996;74:452–466.
60. Rieder F, Kessler S, Sans M, et al. Animal models of intestinal fibrosis: new tools for the understanding of pathogenesis and therapy of human disease. *Am J Physiol Gastrointest Liver Physiol.* 2012;303:G786–G801.
61. Hollanders K, Van Bergen T, Kindt N, et al. The effect of AMA0428, a novel and potent ROCK inhibitor, in a model of neovascular age-related macular degeneration. *Invest Ophthalmol Vis Sci.* 2015;56:1335–1348.
62. Jiang C, Huang H, Liu J, et al. Fasudil, a Rho-kinase inhibitor, attenuates bleomycin-induced pulmonary fibrosis in mice. *Int J Mol Sci.* 2012;13:8293–8307.